Supplementary Information:

Experimental Section

Calixarene molecules were synthesized in-house according to (p-sulfonatocalix[4]arene) ref. S1 and (p-phosphonatocalix[4]arene) ref. S2.

Samples were collected by filtration onto 0.22 µm membranes. The solids were washed with ultrapure water and dried in a desiccator. Subsequently, a portion of the filter paper was placed onto carbon-coated stub and stored in a desiccator. The samples were gold sputtered prior to viewing in a Philips XL30 scanning electron microscope. Larger, 4 L batches were prepared at ambient temperature and magnetically stirred for 3 hours prior to allowing the solids to settle overnight. The solids were decanted, washed and filtered prior to drying in a dessicator. For TEM, the solids were fixed in resin and then ultramicrotomed into thin sections prior to viewing in a Jeol 2011 TEM at 200kV.

The solids collected from the large 4 L batch were analysed on a Bruker D8 Advance using Cu K_a radiation on a low background holder spinning at 30 rpm. The 2 theta range was 15-50 degrees with a step size of 0.001 ° and a divergence slit of 0.3 °. A LynxEye detector was used.

The zeta potential was measured using the Malvern NanoZeta ZS and a plastic zeta cell on particles in the solution they were formed in, at a phosphonated calixarene concentration of 0.013 mM.

AFM experiments were performed on a PicoPlus using a standard silicon nitride cantilever with a flow-through cell attachment. The same procedure was used for all samples. A freshly cleaved mineralogical barium sulfate sample was fixed to a metallic stub and the flow cell was flushed with filtered ultrapure water (resistivity >18 MΩ cm) using a precision, dual syringe pump run at 0.2 mL/min and Gelman 0.2 µm Supor® membrane filters attached to the syringes. One syringe had the water replaced with barium chloride solution (0.1 mM) and the other with sodium sulfate solution (0.1 mM). This was then flushed through the cell at a rate of 0.2mL/min as per the water. Finally, the barium chloride solution was replaced with a solution containing barium chloride plus the calixarene at a known concentration and the sodium sulfate solution was topped up as necessary. This was then flushed through the cell at a rate of 0.2mL/min. For atomic resolution images, the pump was stopped and the system allowed to equilibrate while taking images.

Unseeded, de-supersaturation curves were obtained using a glass reactor kept at 25°C by a water bath and monitored using a conductivity probe (WTW LF 197 Conductivity meter). An overhead stirrer (150 rpm) kept the solids in suspension. The method of precipitation is the same as described in previous publications[S3, S4, S5] and consisted of equilibrating 0.249 mM $BaCl_2$ then adding 1 mol equivalent of Na_2SO_4 solution to initiate crystallization. The total volume for all experiments was 201 mL. The linear region of the de-supersaturation curve (graph of conductivity versus time) was used to calculate the observed de-supersaturation rate. The pH for all experiments was 6.0 except where specified. The calixarene was prepared as a stock solution of 1000 ppm and the desired volume was added to the barium chloride solution prior to the addition of sulfate (keeping the total volume constant by adjusting the water addition). The de-supersaturation rate was found to have an error of ~10%.

The supersaturation in this manuscript is defined such that $S = c/c_o$ where c is the concentration of the ion and c_o is the equilibrium solubility concentration. When the ions forming the crystallizing salt are present at 1:1 ratios and the activity of the ions is ~1, this is reasonably accurate. This approximation has been made because we do not know the extent of barium ion complexation with the calixarene molecules in question. The % inhibition is also calculated based on the following normalized equation:

$$\%\text{Inhibition} = 100*[(k_0-k)/k_0] \qquad -(1)$$

where k_0 is the de-supersaturation rate, for the control run (absence of impurity) and k is the de-supersaturation rate, for the experiment with impurity present.

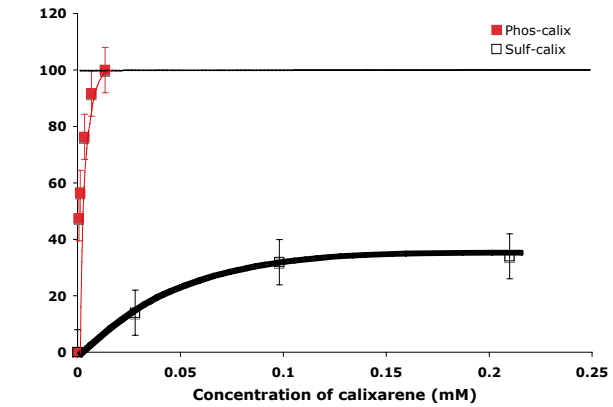

Fig. S1 %inhibition of barium sulfate crystallization derived from conductivity experiments for the two calixarene molecules. Filled squares correspond to the *p*-phosphonatocalix[4]arene and open squares correspond to the *p*-sulfonatocalix[4]arene

Morphology of particles

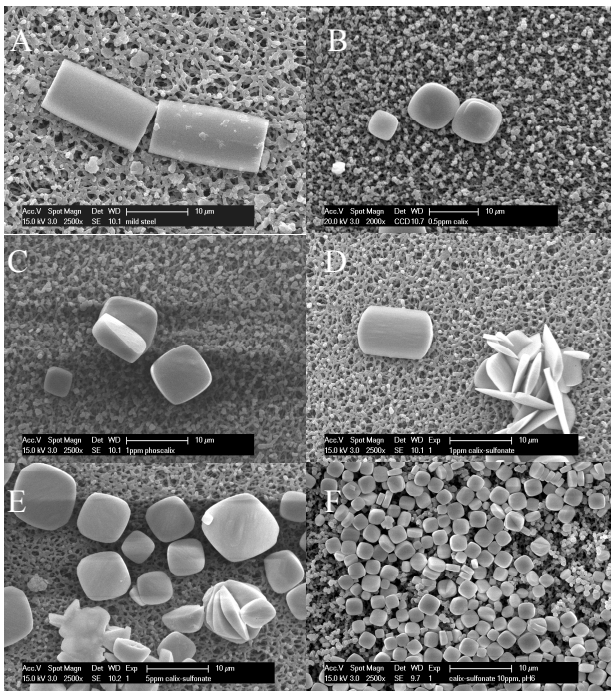

Fig S2. SEM images of barium sulfate formed in the presence of phosphonated calixarene 2 A) 0 mM B) 0.0007 mM and C) 0.0013 mM and in the presence of sulfonated calixarene 1 D) 0.0015 mM E) 0.0073 mM and F) 0.0145 mM

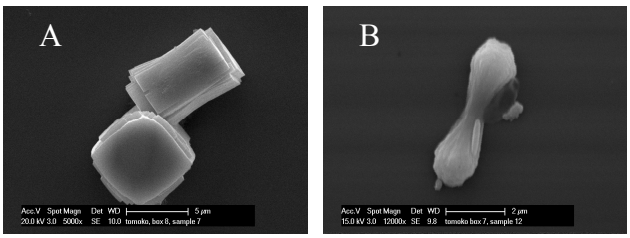

Fig S3. Barium sulfate particles formed in the presence of A) 0.015 mM, and B) 0.030 mM p-sulfonatocalix[4]arene (A was conducted at a lower barium sulfate concentration of 0.05 mM while B was at 0.25 mM $BaCl_2$ and Na_2SO_4)

SAED

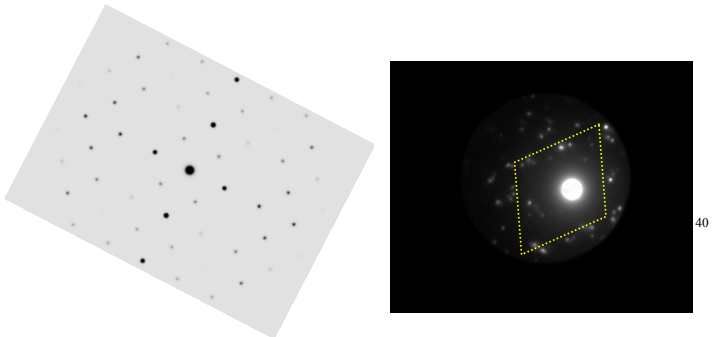

Fig. S4 Predicted SAED for the (100) zone (using Crystal Diffract®) and actual SAED showing the alignment is consistent with the (100) zone

Simulated AFM image

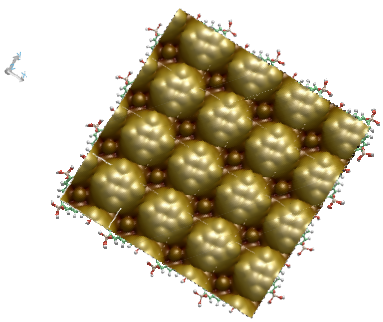

Fig. S5 Simulated AFM image of *p*-phosphonato calix[4]arene bilayer viewed down the *c*-axis

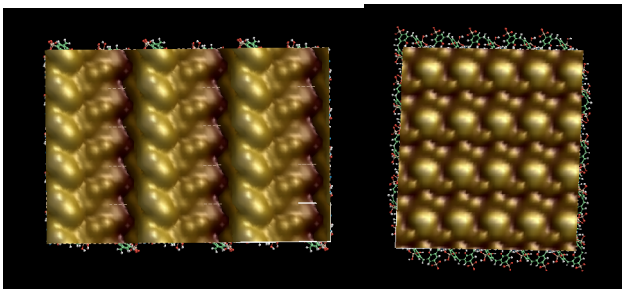

(001) form 2 (010) form 2

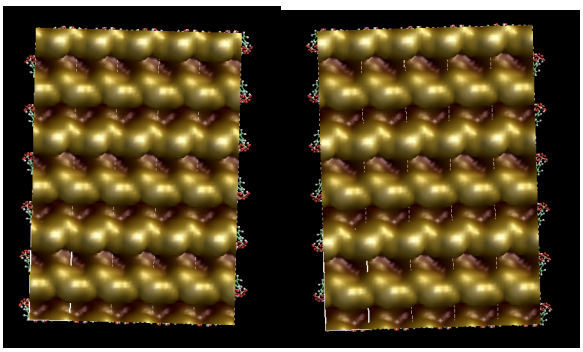

(010) form 1 (100) form 1

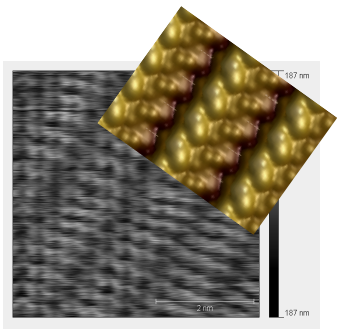

Fig. S6 Simulated AFM images of calcium complexes of *p*-phosphonato calix[4]arene

References

[S1] S. Shinkai, K. Araki, T. Tsubaki, T. Arimura, O. Manabe *J. Chem. Soc. - Perkins Trans.* **1987** *1(11)* 2297-2299.

[S2] A. D. Martin, A. N. Sobolev, M. A. Spackman, C. L. Raston, *Crystal Growth & Design* **2009** *9* 3759-3764.

[S3] F. Jones, J. Clegg, A. Oliviera, A. L. Rohl, M. I. Ogden, G. M. Parkinson, A. M. Fogg, M. M. Reyhani (2001), *CrystEngComm* **40** 1.

[S4] S. R. Freeman, F. Jones, M. I. Ogden, A. Oliviera, W. R. Richmond (2006), *Crystal Growth & Design* **6** 2579.

[S5] F. Jones, W. R. Richmond, A. L. Rohl (2006), *J. Phys. Chem. B* **110** 7414.